한국소성가공학회 '99추계학술대회 논문집 pp.53~62

유한 탄소성 쉘 문제를 위한 h-Adaptive 유한요소법

한정석* · Peter Wriggers**

*서울대학교 기계설계학과

**Institut für Baumechanik und Numerische Mechanik, University of Hannover

Towards h–Adaptive FE-procedures for Shell Problems in Finite Elasto–Plasticity

C.-S. HAN* AND P. WRIGGERS**

*Dept. of Mechanical Design and Production Eng., Seoul National University, Korea

**Institut für Baumechanik und Numerische Mechanik, University of Hannover, Germany

1 Introduction

Since in FE-simulations the structure has to be discretized an spatial discretization error is inevitable in general. The aim of an h-adaptive procedure is to control this discretization error. An h-adaptive FE-procedures for nonlinear problems can be divided into the components FE-analysis, error estimation/indication, mesh generation and the transfer of the current state form one mesh to the other, which is also known from bulk forming processes as rezoning procedure to avoid ill-shaped elements during the deformation process [1].

In this paper shell problems in finite elasto-plasticity are considered. For this the components FE-analysis - described in more detail in [2] and [3], error indication on basis of the Superconvergent Patch Recovery [4] and the transfer of the current state are briefly described. Especially the transfer of the current state, is taken here into consideration. Adaptive methods applying such transfers are described in [5], [6] for small strain problems, in [7], [3] also large plastic strains are taken into account. The problematic nature of this transfer for elasto-plastic shell problems in the context of an adaptive procedure is outlined and two h-adaptive strategies are proposed, one employing and one avoiding this transfer. These strategies are finally applied in numerical examples to illustrate the performance of the procedures.

2 Components of the h–Adaptive FE-Method

2.1 FE-Formulations

Shell Element. The shell formulation is based on a so called five parameter *quasi-Kirchhoff-theory* derived in more detail in [2] and is applicable to structural problems with finite rotations and large strains.

An arbitrary point in the deformed shell space of the current configuration is determined by $\mathbf{x}(\xi^1, \xi^2, \zeta) = \boldsymbol{\phi}(\xi^1, \xi^2) + \zeta \mathbf{d}(\xi^1, \xi^2)$, where $\boldsymbol{\phi}$ denotes the shell mid-surface and $\mathbf{d}$ an inextensible director of unit length expressed in terms of two rotation angles β_1 and β_2, see [2]. The curvilinear base vectors are given by

$$\mathbf{g}_\alpha = \boldsymbol{\phi}_{,\alpha} + \zeta \mathbf{d}_{,\alpha} = \mathbf{a}_\alpha + \zeta \mathbf{d}_{,\alpha} \ , \quad \alpha = 1, 2 \ , \quad \mathbf{g}_3 = \mathbf{d}. \tag{1}$$

A strain measure with respect to the reference configuration is provided by the right Cauchy-Green tensor $\mathbf{C}$ with $C_{ij} = \mathbf{g}_i \cdot \mathbf{g}_j$ being the covariant components of $\mathbf{C}$. Herein the quadratic terms in ζ have been neglected due to the thin shell limit.

From $\mathbf{C}$ we can easily obtain the Green–Lagrange strain by $E_{ij} = \frac{1}{2}(C_{ij} - \delta_{ij})$, where the Kirchhoff constraint $E_{\alpha 3} = 0$ is imposed to suppress shear strains. This condition is incorporated in the finite element formulation by adding this constraint into a penalty term of the variational form

$$\int_{B_o} S_{\alpha\beta}\delta E_{\alpha\beta} dV + c_{pen} \int_{B_o} E_{\alpha 3}\delta E_{\alpha 3} dV = \int_{B_o} \rho_o \mathbf{b} \cdot \delta\mathbf{u}\, dV + \int_{\partial B_o} \mathbf{t}_o \cdot \delta\mathbf{u}\, dA \tag{2}$$

with the shear penalty parameter c_{pen}. Within this shell model we use the classical plane stress assumption $S_{33} = 0$ to describe the material behavior. Thus with the additional condition $E_{\alpha 3} = 0$ the constitutive equations are fully described by the plane stress state.

Finite Elasto-Plasticity. The material behavior is considered to be isotropic elasto–plastic and the analysis is employed by the usual multiplicative decomposition of the deformation gradient

$$\mathbf{F} = \mathbf{F}^e \mathbf{F}^p. \tag{3}$$

A local free energy function Ψ is assumed in which the hardening mechanisms are decoupled from the elastic deformation $\Psi(\boldsymbol{\varepsilon}^e, \alpha) = \mathcal{W}(\boldsymbol{\varepsilon}^e) + \mathcal{H}(\alpha)$, with $\boldsymbol{\varepsilon}^e = \frac{1}{2} ln(\mathbf{b}^e)$ and $\mathbf{b}^e = \mathbf{F}^e \mathbf{F}^{e^T}$. Moderate large elastic strains are considered in $\mathcal{W}$ common for metal plasticity with $\mathcal{W} = \frac{1}{2}\boldsymbol{\varepsilon}^e \cdot \mathbb{C}\boldsymbol{\varepsilon}^e$, where in $\mathbb{C}$ the elastic moduli are contained. In addition a potential function for the hardening variables is defined with $\mathcal{H} = \frac{1}{2} H\alpha^2$, with the hardening module H.

The principal Kirchhoff stresses τ_i are work conjugate to the elastic principal logarithmic strains ε_i^e hence the stress response can be described with $\tau_i = \partial_{\varepsilon_i^e} \mathcal{W}$ and $q = -H\alpha$. The v. Mises yield criterion is applied

$$\Phi(\mathbf{s}, q) = \frac{3}{2} tr(\mathbf{s}^2) - (\sigma_y - q)^2 \leq 0 \tag{4}$$

with the deviator of the Kirchhoff stresses $\mathbf{s}$ yielding the associated flow rule via principle of maximum dissipation, e.g. [8]. After some steps ([9], [10]) we arrive at the eigenvalue problem in the current configuration

$$\begin{aligned} \mathbf{C}^{p^{-1}} \mathbf{N}_i &= (\lambda_i^e)^2 \mathbf{C}^{-1} \mathbf{N}_i \\ \mathbf{N}^i \mathbf{C} &= (\lambda_i^e)^2 \mathbf{N}^i \mathbf{C}^p, \end{aligned} \tag{5}$$

where $\mathbf{N}_i$ and $\mathbf{N}^i$ are the dual co– and contravariant eigenvectors associated with $(\lambda_i^e)^2$. With the principal stretches $(\lambda_i^e)^2$ the return mapping procedure described below can be applied via $\varepsilon_i^e = \frac{1}{2} ln(\lambda_i^e)^2$. The strains and stresses can be represented with these eigenvectors in terms of the reference configuration by

$$\mathbf{C}^p = \sum_{i=1}^{3} \mathbf{N}_i \otimes \mathbf{N}_i\ , \quad \mathbf{C} = \sum_{i=1}^{3} (\lambda_i^e)^2 \mathbf{N}_i \otimes \mathbf{N}_i\ , \quad \mathbf{S} = \sum_{i=1}^{3} \frac{\tau_i}{(\lambda_i^e)^2} \mathbf{N}^i \otimes \mathbf{N}^i, \tag{6}$$

where $\mathbf{N}_i$ and $\mathbf{N}^i$ obey the relations $\mathbf{N}^i \mathbf{N}_k = \delta_k^i$ and $\mathbf{N}_i \cdot \mathbf{C}^{p^{-1}} \mathbf{N}_i = 1$.

The *exponential return mapping* is formulated in principal axes for the plane stress state. Considering a time interval $[t_n, t_{n+1}]$ we start by $\mathbf{C}_{n+1}$ and $\mathbf{C}_{n+1}^{p^{tr}} = \mathbf{C}_n^p$, $\alpha_{n+1}^{tr} = \alpha_n$ and solve (5) with these values. The implicit integration $(t_{n+1} - t_n)\dot{\gamma} \longrightarrow \Delta\gamma$ yields after some steps to the stresses $\boldsymbol{\tau}_{n+1}$ and the hardening variable α_{n+1} as functions of the consistency parameter $\Delta\gamma$. Contrary to the three dimensional case where $\Delta\gamma$ can be eliminated directly, $\Delta\gamma$ is computed here via Newton iteration from

$$\Phi(\boldsymbol{\tau}(\Delta\gamma), \alpha(\Delta\gamma)) = 0. \tag{7}$$

For an explicit illustration of this mapping the reader is referred to i.e. [3].

2.2 Error Indication for Elasto-Plastic Shells

The elasto-plastic error indication is applied to large strain problems and derived with respect to the current configuration, in which the return mapping procedure is referred to by ε_i^e and τ_i [3]. All quantities are then pulled back again into the reference configuration where the indication is evaluated via Superconvergent Patch Recovery [4].

First we consider the free elastic energy $\mathcal{W}$ as norm

$$\|\boldsymbol{\tau}\|_{\mathcal{W}}^2 = \int_\Omega \boldsymbol{\tau} \cdot \mathbb{C}^{-1}\boldsymbol{\tau}\, d\Omega. \tag{8}$$

To determine the error of the finite element solution $\boldsymbol{\tau}_h$ we compare it with the exact solution $\boldsymbol{\tau}$ and define the error in the stresses $\mathbf{e}_\tau = \boldsymbol{\tau}_h - \boldsymbol{\tau}$.

An upper bound of this error in $\|.\|_{\mathcal{W}}$ can be found following [11] in some steps

$$\|\mathbf{e}_\tau\|_{\mathcal{W}}^2 \leq \int_\Omega (\boldsymbol{\varepsilon}^{e^{tr}} - \boldsymbol{\varepsilon}_h^{e^{tr}}) \cdot (\boldsymbol{\tau} - \boldsymbol{\tau}_h) d\Omega, \tag{9}$$

with the elastic logarithmic trial strain $\boldsymbol{\varepsilon}^{e^{tr}}$. To be able to evaluate all quantities in the reference configuration we have to pull back $\boldsymbol{\tau}$ and $\boldsymbol{\varepsilon}^{e^{tr}}$ by

$$\mathbf{S} = \mathbf{F}^{-1}\boldsymbol{\tau}\mathbf{F}^{-T} \quad , \quad \tilde{\mathbf{E}}^{e^{tr}} = \mathbf{F}^T\boldsymbol{\varepsilon}^{e^{tr}}\mathbf{F} \tag{10}$$

yielding the error indication

$$\|\mathbf{e}_\tau\|_{\mathcal{W}}^2 \approx \int_\Omega (\tilde{\mathbf{E}}_\star^{e^{tr}} - \tilde{\mathbf{E}}_h^{e^{tr}}) \cdot (\mathbf{S}_\star - \mathbf{S}_h) d\Omega \tag{11}$$

with the recovered values $\tilde{\mathbf{E}}_\star^{e^{tr}}$ and $\mathbf{S}_\star$ by the SPR, see [4] for details. The recovery procedure is done hereby in the tangential coordinate system of the shell mid surface. An expansion of (11) to the free energy Ψ as error norm is easily done with

$$\|\mathbf{e}_{(\tau,\alpha)}\|_\Psi^2 \approx \int_\Omega (\tilde{\mathbf{E}}_\star^{e^{tr}} - \tilde{\mathbf{E}}_h^{e^{tr}}) \cdot (\mathbf{S}_\star - \mathbf{S}_h) + H(\alpha_\star - \alpha_h)^2 d\Omega. \tag{12}$$

Other norms are considered e.g. in [12], [13] and [14] where a different approach is applied.

2.3 Transfer of State Variables

If a procedure of evolving meshes is considered the state variables defining the current state of deformation have to be transferred from one mesh to the other. This procedure is especially common for forming processes, where the elements can get heavily ill-shaped during the deformation, see e.g. [1]. For this at least the nodal $\mathbf{v} = (\mathbf{u}, \boldsymbol{\beta})$ and internal variables $\mathbf{i} = (\mathbf{C}^p, \alpha)$ updated in each load step have to be transmitted to the new mesh. Note that transferring all available data $\mathbf{u}, \boldsymbol{\beta}, \mathbf{C}, \mathbf{S}, \mathbf{C}^p, \alpha, ...$ yields in general to an inconsistent relation in between these data in the new mesh.

Several procedures for this transfer are possible (e.g. [5], [6], [7]), the procedure followed here shall be described with fig. 1. The internal variables are projected via SPR to the nodes in the old mesh h, fig. 1(a). Nodal and internal variables are then transmitted to the nodes in the new mesh $h+1$, fig. 1(b). Hereby the nodal displacements are transmitted by Hermitian interpolation, see [3]. Finally the internal variables are interpolated to the Gauss points, fig. 1(c).

Independent of the followed transfer procedure an error in the transfered data is not avoidable, due to the transfer itself and due to the fact, that the data in the old mesh

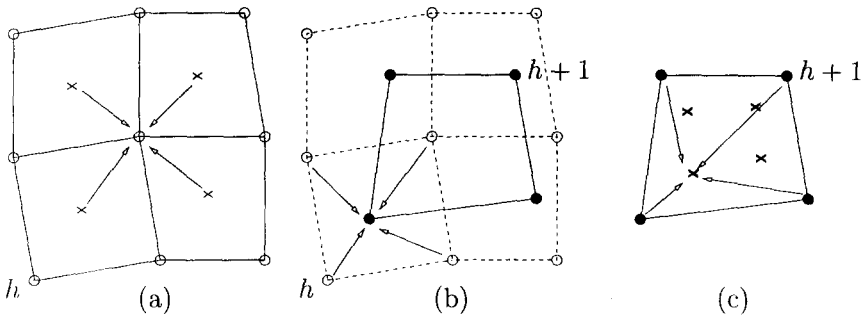

Figure 1: Transfer of history variables.

are already affected with a discretization error. Therefore after the transfer the discrete equilibrium of (2) is violated $\mathbf{G}^{h+1}(\mathbf{v}^{trans}, \mathbf{i}^{trans}) \neq \mathbf{0}$. By iterating of the nodal variables $\mathbf{v}$ to equilibrium with the Newton-Raphson scheme

$$\mathbf{G}^{h+1}(\mathbf{v}^{h+1}, \mathbf{i}^{trans}) = \mathbf{0} \tag{13}$$

the current state in the new mesh is obtained. It should be mentioned here that the tangential stiffness matrix computed with these transfered values can be badly conditioned especially in case of large strains. In addition we also may have a large residuum therefore the solution of (13) is not easy to achieve and may require considerably more iterations as usual.

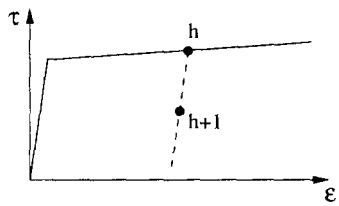

Figure 2: Stresses before and after an adaptive step, if $\varepsilon_h > \varepsilon_{h+1}$.

In the numerical equilibrium state of the new mesh (13) the strains differ in general from those of the old mesh, whereas the internal variables $\mathbf{i}^{trans}$ remain fixed after the transformation to the new mesh. A consequence in case of smaller strains in the new mesh is illustrated in fig. 2, there especially in metal plasticity strong decreases in the stresses can occur. This effect will evolve stronger when the deformation proceeds, since the elastic strains become smaller in relation to the plastic strain yielding a stronger unloading due to the unchanged plastic strains. Hence especially the stresses in view of $\tau_i = \partial_{\varepsilon_i^e} \mathcal{W}$ after this transfer are not reliable and in a strict sense a new source of error is established with this transfer.

In this context the approach described in [7] seems more attractive at the first glance since in there the elastic deformation gradient $\mathbf{F}^e$ is used to transmit $\mathbf{C}^p$ to avoid the reduction of the elastic strains described before. A supposition for this approach however is a sufficient good mapping of the deformation before the iteration to (13) is started. This is required since an iteration of $\mathbf{v}$ to (13) with a constant $\mathbf{F}^e$ or $\boldsymbol{\varepsilon}^e$ can not be guaranteed to achieve a self-consistent state. Due to the sensibility of the considered thin walled structures and the correlation between $\mathbf{u}$ and $\boldsymbol{\beta}$ the transmition by the discrete values of $\mathbf{u}$ and $\boldsymbol{\beta}$ does not yield a good approximation of the deformation with respect to (13) particularly when the deformation is strongly affected to bending. Hence in numerical tests this transformation did not yield to a better performance than the approach described before.

3 Adaptive Strategies

The combination of the ingredients of an adaptive FE-method mentioned in the introduction to an adaptive procedure is described in the following. To control the discretization error a criterion for remeshing has to be defined. Since the optimal mesh changes with the deformation the data of the current state of the structure has to be transferred from one mesh to the other in order to achieve an optimal exploitation of the computational resources. The adaptive procedure for evolving meshes during deformation is illustrated in fig. 3. As a criterion

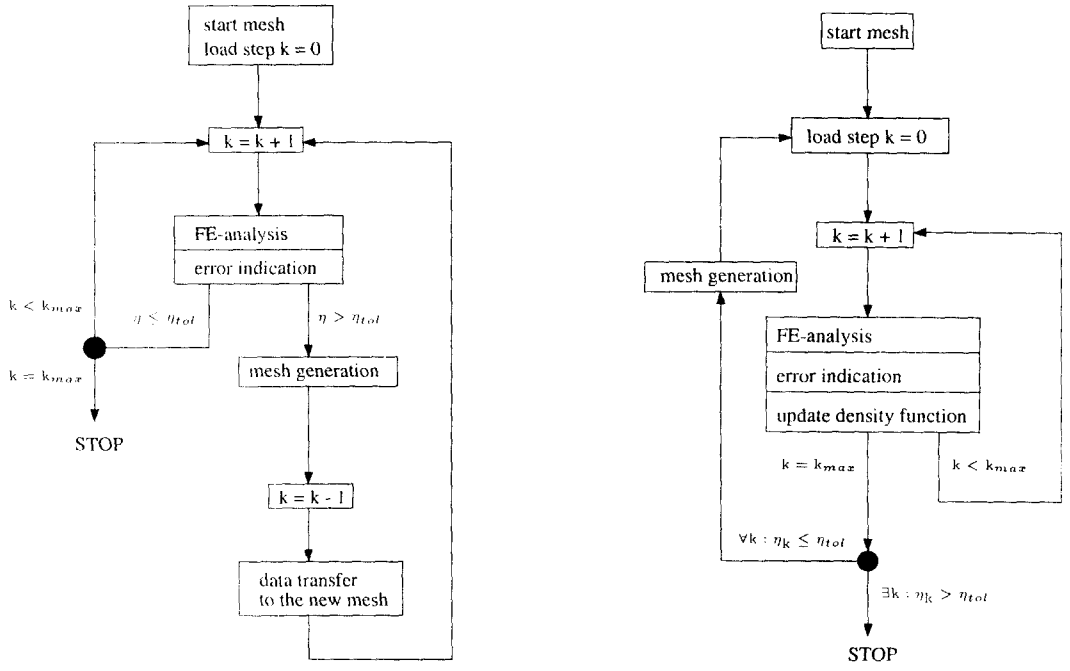

Figure 3: Adaptive procedures with and without transfer.

for remeshing the relative error

$$\eta = (\|\mathbf{e}\|^2/\|\mathbf{e}\|^2 + \|\mathbf{u}\|^2)^{\frac{1}{2}} \tag{14}$$

is evaluated which has to be under a given tolerance η_{tol}. To obtain a mesh fulfilling the required tolerance $\eta \leq \eta_{tol}$ a local predicted element size yielding a even distribution of the error is computed by

$$h^e_{new} = h^e_{old} \frac{e_m}{\|\mathbf{e}_\tau\|_e} \quad \text{with} \quad \|\mathbf{e}\|_e \leq e_m = \eta_{tol}[(\|\mathbf{e}_\tau\|^2 + \|\boldsymbol{\tau}_h\|^2)/n_{el}]^{\frac{1}{2}}. \tag{15}$$

With this description of the element density the new mesh is generated.

If history independent problems are considered the transfer can be done without severe problems – excluding singular loading points – by projecting the deformation to the new mesh and iterating the nodal values to equilibrium. If history dependent problems are considered internal variables have to be transferred which can not be done in general without loss of accuracy, as described in section 2.3. To avoid a new source of error a second strategy is proposed in which no transfer of variables is needed, see right diagram in fig. 3. Here for every remeshing the computation starts again from the first load step. The density of the elements

in the mesh can be defined then by the smallest local element size during the computation of all load steps $k = 1, ..., k_{max}$

$$h^e = \min_k \{h_k^e\} \ . \tag{16}$$

The procedure ends if all load steps are computed with a mesh fulfilling the prescribed tolerance $\eta_k \leq \eta_{tol}$, $\forall k$.

4 Numerical Examples

Pinched cylinder. In this problem the elasto-plastic deformation of the pinched cylinder widely known from the literature is considered. The adaptive solutions are carried out for tolerances of 15 and 10% with respect to $\|.\|_{\mathcal{W}}$ as error norm. The applied load and the relative error of the computations are presented in fig. 4, additionally in the right picture of fig. 4 the number of elements used in each adaptive mesh are shown. For displacement

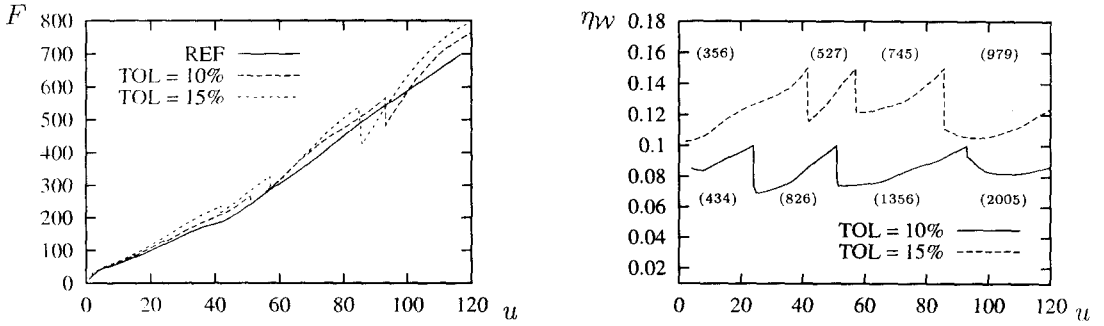

Figure 4: Applied loads and relative error over the load steps with transfer.

Figure 5: Evolving meshes in the deformed configuration with a $TOL = 15\%$.

loading up to $u = 80.0$ we can see that the adaptive computations are in good accordance with the reference solution, especially after remeshing when the structure gets softer and the applied force decreases. Between $u = 80$ and 100 all adaptive runs show decreases which are over-proportional in relation to the applied forces. For reasons concerning this strong decrease we have of course to think about the error made by transferring $\mathbf{C}_p$ and α. This error is especially severe in this problem due to the plastification in the kink which is characteristic for this pinched cylinder problem. The results of the computations are strongly dependent on the size of the elements used in the region of this kink, see also [15]. The structure exhibits large bending strains at this kink yielding a plastic 'hinge' for large u. Hence the results of

the computations will be very sensitive to the errors made by transferring $\mathbf{C}_p$ and α within this region. If the mesh is finer the errors made by transferring the history data will be smaller and hence the descent of the applied force is smaller, too, see fig.4 left diagram.

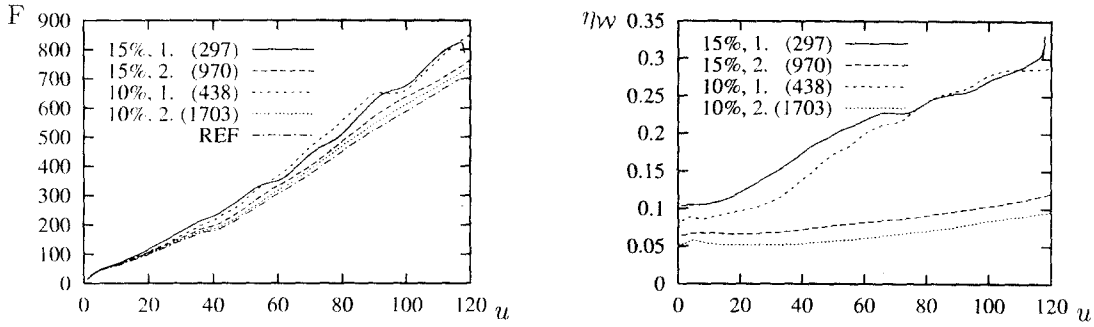

Figure 6: Applied load and relative error η_W without transfer.

Figure 7: Meshes in the final configuration with a $TOL = 15\%$ without transfer.

As comparison the same problem is computed with the strategy without transfer of the state variables. As initial meshes adaptive discretizations fulfilling the tolerance in the first load step are chosen. To undergo both tolerances (15 and 10%) over all load steps only one further remeshing is needed. In fig. 6 the applied load and the relative error η_W are shown. About the same number of elements are needed as with the simulation with transfer of the state variables in the last adaptive mesh.

Deep drawing of a sheet. In the 2nd example the deep drawing of a sheet is simulated as illustrated in fig. 8. Since very large plastic strains are expected in this example only the strategy without transfer is considered. The rigid tools are described with several NURBS–surfaces, the contact routine is described by a frictionless penalty formulation. The data for the material and definition of the master surfaces can be found in [16]. In the simulation die and blank holder are positioned to each other in a distance of $d = 0.1$. The punch is pushed after the first touch with the sheet in intervals of $\Delta u = 0.05$ till it has reached the final position $u = 50.0$. The adaptive simulations are performed for 15% and 10% with respect to $\|.\|_\psi$. The sum over the vertical contact forces of the die and the relative error with respect to $\|.\|_\psi$ of the simulations are plotted in fig. 9. Three meshes were needed to undergo the tolerances of 15% and 10%. In fig. 10 the last mesh in the final configuration with $TOL = 10\%$ full-filling the prescribed tolerance of 10% is shown.

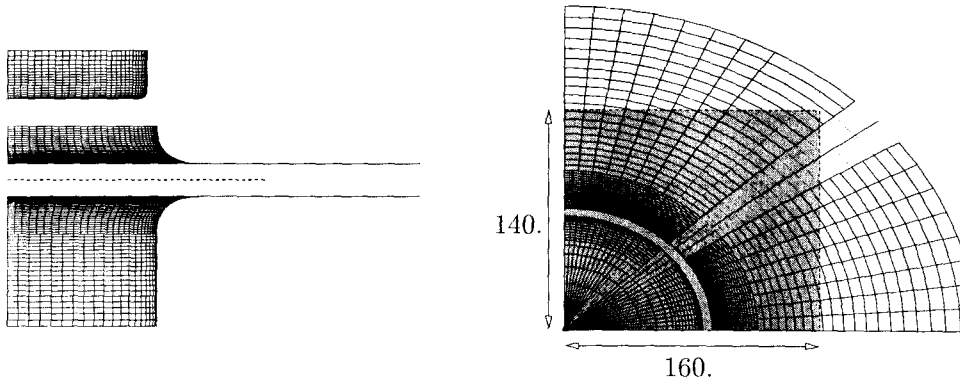

Figure 8: Deep drawing of a sheet with a NURBS-description of the tools.

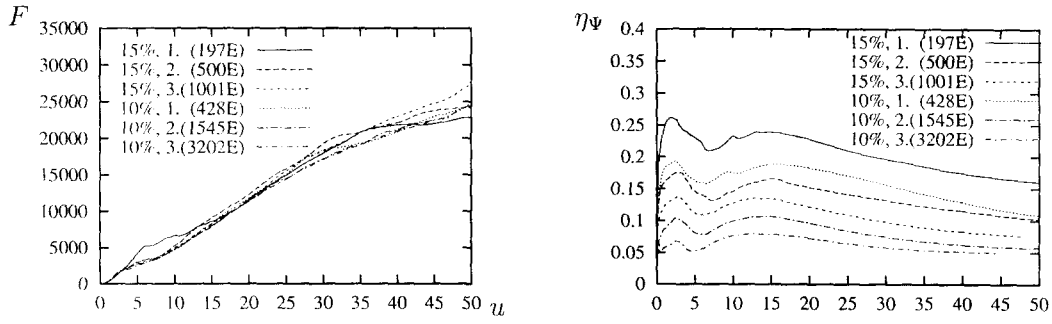

Figure 9: Vertical applied contact force and relative error η_Ψ.

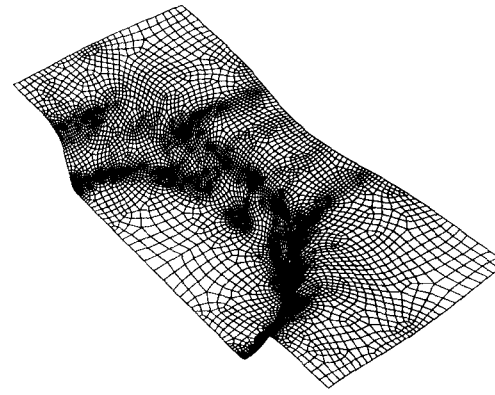

Figure 10: Last mesh in the final configuration with $TOL = 10\%$.

5 Conclusion

In this paper the components FE-analysis, error indication and transfer of the current state of an h-adaptive FE-method were briefly described and two strategies were proposed combining the components to an h-adaptive procedure.

As described strong decreases in the stresses have to be taken into account when applying the transfer of the current state for history dependent materials, especially in case of metal plasticity. The first example illustrates that this local decreases can yield a strong response also on overall structural context. Hence considerable errors can occur with the strategy of

evolving meshes particularly for large plastic strains due to the transfer of the current state. Note that this error also affects the error in the space discretization and yields higher error indications. Although by applying the second strategy all load steps have to be computed for every adaptive discretization, this strategy seems to be more appropriate for the considered large strain analysis since for shell problems ill-formed element geometries due to the deformation do not have to be considered as a severe problem in general as in the simulations of bulk form processes.

Acknowledgement–The Authors would like to thank Prof. Soo-Ik Oh for his generous support and advises.

References

[1] S. I. Oh, J. P. Tang, and A. Badawy. Finite element mesh rezoning and its applications to metal forming analysis. *Int. J. Mech. Sci*, 22:583–594, 1980.

[2] R. Eberlein and P. Wriggers. Finite Element Formulations of Five and Six Parameter Shell Theories Accounting for Finite Plastic Strains. In *Computational Plasticity, Fundamentals and Applications*, Owen, D. R. J. and Onate, E. and Hinton, E. (Eds.), Barcelona, 1997. CIMNE. 1898–1903.

[3] C.-S. Han and P. Wriggers. An h–adaptive method for elasto–plastic shell problems. *Comp. Meth. App. Mech. Eng.*, 1999. accepted for publication in Comp. Meth. App. Mech. Eng. 1999.

[4] O.C. Zienkiewicz and J.Z. Zhu. The superconvergent patch recovery and *a posteriori* error estimates. part 1: the recovery technique. *Int. J. Num. Meth. Eng.*, 33:1331–1364, 1992.

[5] M. Ortiz and J. Quigley. Adaptive mesh refinement in strain localization problems. *Comp. Meth. App. Mech. Eng.*, 90:781–804, 1987.

[6] D. Perić, Ch. Hochard, M. Dutko, and D.R.J. Owen. Transfer operators for evolving meshes in small strain elasto–plasticity. *Comp. Meth. App. Mech. Eng.*, pages 331–334, 1996.

[7] N.-S. Lee and K.-J. Bathe. Error indicators and adaptive remeshing in large deformation finite element analysis. *Finite Elements in Analysis and Design*, 16:99–139, 1994.

[8] J.C. Simo and T.J.R. Hughes. *Computational Inelasticity*. Springer, 1998.

[9] A. Ibrahimbegovic. Finite Elastoplastic Deformations of Space–Curved Membranes. *Comp. Meth. App. Mech. Eng.*, 119:371–394, 1994.

[10] C. Miehe. A theoretical and computational model for isotropic elastoplastic stress analysis in shells at large strains. *Comp. Meth. App. Mech. Eng.*, 155:193–233, 1998.

[11] C. Johnson and P. Hansbo. Adaptive finite element methods for small strain elasto–plasticity. In D. Besdo and E. Stein, editors, *Finite inelastic deformations – Theory and Applications*. Springer, 1992.

[12] D. Perić, J. Yu, and D.R.J. Owen. On error estimates and adaptivity in elastoplastic solids: Applications to the numerical simulation of strain localization in classical and Cosserat continua. *Int. J. Num. Meth. Eng.*, 37:1351–1379, 1994.

[13] K.M. Mathisen, I. Tiller, K.M. Okstad, and O.S. Hopperstad. On adaptive non-linear shell analysis. In E. Onate S. Idelsohn and E. Dvorkin, editors, *Computational Mechanics, New trends and Applications*. CIMNE, Barcelona, Spain, 1998.

[14] L. Gallimard, P. Ladevèze, and J.P. Pelle. Error estimation and adaptivity in elastoplasticity. *Int. J. Num. Meth. Eng.*, 39:189–217, 1996.

[15] R. Hauptmann and K. Schweizerhof. A systematic developement of 'solid–shell' element formulation for linear and non–linear analysis employing only displacement degrees of freedom. *Int. J. Num. Meth. Eng.*, 42:49–69, 1998.

[16] C.-S. Han. *Eine h-adaptive FE-Methode für elasto–plastische Schalenprobleme in unilateralem Kontakt.* Forschungs– und Seminarberichte IBNM Universität Hannover, Bericht–Nr. F99/1, 1999.